Electrospray Ionization Mass Spectrometry Studies on the Mechanism of Hydrosilylation of Terminal Alkynes Using an N-Heterocyclic Carbene Complex of Iridium, Allow Detection/ Characterization of All Reaction Intermediates[⊥]

Cristian Vicent,[†] Mónica Viciano,[‡] Elena Mas-Marzá,[‡] Mercedes Sanaú,[§] and Eduardo Peris*,[‡]

Servicios Centrales de Instrumentación Científica (SCIC), Universitat Jaume I, Avenida Vicente Sos Baynat s/n, Castellón, E-12071, Spain, Departamento de Química Inorgánica y Orgánica, Universitat Jaume I, Avenida Vicente Sos Baynat s/n, Castellón, E-12071 Spain, and Departamento de Química Inorgánica, Universitat de Valencia, C/Dr. Moliner s/n, Burjassot-Valencia, E-46100 Spain

Received March 13, 2006

A new pyridine-4,5-dichloroimidazol-2-ylidene complex of Ir(I) has been obtained, and its catalytic activity toward hydrosilylation of phenylacetylene and 4-aminophenylacetylene has been studied. The addition of $HSiMe_2Ph$ to the latter Ir(I) species afforded the corresponding Ir^{III}-NHC hydrosilylated species, whose molecular structure was determined. This species and its nonchlorinated analogue have been used as catalyst of a series of reactions designed for elucidating the catalytic processes. The mechanism of the catalytic hydrosilylation of phenylacetylene has been studied by means of electrospray ionization mass spectrometry (ESI-MS) and tandem MS/MS, allowing the detection of all the reaction intermediates leading to both the hydrosilylation and the dehydrogenative-silylation products. The ratio of the silylation/ hydrosilylation products depends on the excess of phenylacetylene added to the reaction mixture.

Introduction

Transition metal-catalyzed hydrosilylation of unsaturated hydrocarbons such as alkenes or alkynes is a versatile synthetic way to provide organosilicon compounds.[1] The basic mechanistic picture starts from a hydrosilane $MH(SiR_3)$ complex (M = Pd, Co, Ir, Rh) to which the unsaturated hydrocarbon is subsequently coordinated. One of the most widely accepted mechanisms for this catalysis was first reported by Chalk and Harrod in 1965, in which insertion of a coordinated alkene (or alkyne) into a metal−hydrogen bond (*hydrometalation*) is followed by reductive elimination of alkyl (or alkenyl) and silyl ligands to give rise to the hydrosilylation products (Scheme 1, pathway a).[2] An alternative mechanistic description, the so-called modified Chalk−Harrod mechanism, was introduced later and implies that the coordinated alkene (or alkyne) is inserted into a metal−silicon bond (*silylmetalation*), followed by reductive elimination of β-silylalkyl (or β-silylalkenyl) and the hydride ligand to afford the hydrosilylation products (Scheme 1, pathway b).[3] This latter mechanism also accounts for the occasional formation of alkenylsilanes (or alkynylsilanes) in the catalytic dehydrogenative silylation of alkenes (or alkynes).[4−6]

Scheme 1

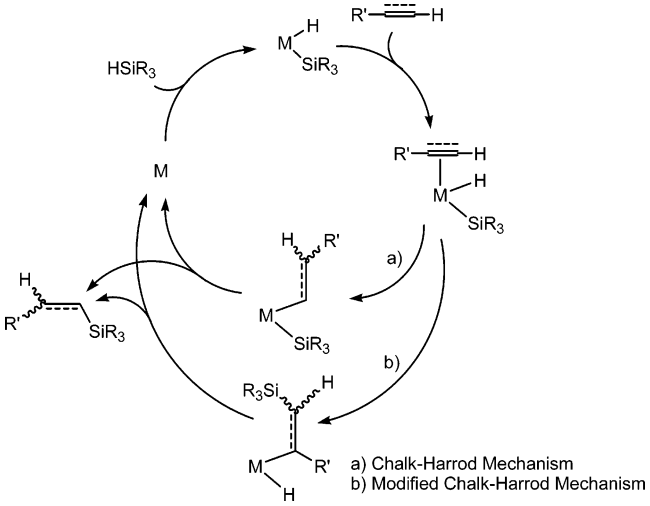

In general, hydrosilylation pathways are dominant for the vast majority of active catalysts, while dehydrogenative silylation processes tend to appear as side reactions, making its mechanistic elucidation complicated. Mechanistic studies of either hydro- or silylation reactions have heavily relied on the

[⊥] This article is dedicated to Dr. Antonio Abad on the occasion of his retirement.

* To whom correspondence should be addressed. E-mail: eperis@qio.uji.es.

[†] SCIC, Universitat Jaume I.

[‡] Departamento de Química Inorgánica y Orgánica, Universitat Jaume I.

[§] Universitat de Valencia.

(1) Ojima, I. *The Chemistry of Organic Silicon Compounds*; Wiley: New York, 1989; p 1479. Ojima, I.; Li, Z.; Zhu, J. *The Chemistry of Organic Silicon Compounds*.; Wiley: New York, 1998; p 1687. Luh, T.; Liu., S. *The Chemistry of Organic Silicon Compounds*; Wiley: New York, 1998; Vol. 2, p 1793.

(2) Harrod, J. F.; Chalk, A. J.; Davies, N. R. *Nature* **1965**, *205*, 280. Chalk, A. J.; Harrod, J. F. *J. Am. Chem. Soc.* **1965**, *87*, 16.

(3) (a) Harrod, J. F., Chalk, A. J., Wender, I., Pino, P., Eds. In *Organic Synthesis via Metal Carbonyls*; Wiley: New York, 1977; Vol. 2, p 673. *(*b) Schroeder, M. A.; Wrighton, M. S. *J. Organomet. Chem.* **1977**, *128*, 345.

(4) Esteruelas, M. A.; Olivan, M.; Oro, L. A.; Tolosa, J. I. *J. Organomet. Chem.* **1995**, *487*, 143. Brookhart, M.; Grant, B. E. *J. Am. Chem. Soc.* **1993**, *115*, 2151. LaPointe, A. M.; Rix, F. C.; Brookhart, M. *J. Am. Chem. Soc.* **1997**, *119*, 906.

(5) Shimizu, R.; Fuchikami, T. *Tetrahedron Lett.* **2000**, *41*, 907.

(6) Jun, C. H.; Crabtree, R. H. *J. Organomet. Chem.* **1993**, *447*, 177.

10.1021/om0602308 CCC: $33.50
Publication on Web 06/15/2006

identification of the organic products formed or by detecting the metal intermediates by spectroscopic techniques such as variable-temperature multinuclear ^{31}P, ^{13}C, and ^{1}H NMR and UV−vis spectroscopies or by theoretical approaches.[7,8] In general, because of the low concentration and transient nature of most of the intermediates involved, their identification has remained a task of great complexity and the information provided is limited except in a few cases.

In this context, soft-ionization mass spectrometry techniques have recently appeared as a breakthrough for the rapid and sensitive characterization of organometallic compounds, since they allow preexisting molecules in solution to be transferred to the gas phase with minimal fragmentation. In particular, electrospray ionization mass spectrometry (ESI-MS) and its tandem version (MS/MS) are rapidly becoming the techniques of choice for solution mechanistic studies in chemistry and biochemistry and for high-throughput screening of homogeneous catalysis reactions.[9]

During the last five years, the interest of our research group focused on the preparation of new N-heterocyclic carbene complexes for homogeneous catalysis.[10] We recently described a series of N-heterocyclic carbene complexes of Rh(I) and Ir(I) that showed catalytic activity in the hydrosilylation of terminal acetylenes and alkenes.[11−13] We observed that our Ir(I) catalysts showed lower efficiency than the related Rh(I) species in terms of both reaction rates and yields. This low efficiency of our Ir^{I}-NHC complexes made us think that the system may be suitable for mechanistic studies, since low rates may provide long-lived reaction intermediates detectable by the conventional spectroscopic techniques. In this sense, we now describe a detailed mechanistic study of the reaction of $HSiMe_2Ph$ with phenylacetylene and 4-aminophenylacetylene catalyzed by an iridium(I) complex with a pyridine-imidazol-2-ylidene ligand using ESI-MS and tandem MS/MS. We also found it convenient to prepare a series of pyridine-4,5-dichloroimidazol-2-ylidene complexes of Ir(I) and Ir(III), to compare their reactivity with the nonchlorinated analogue NHC species.

Scheme 2

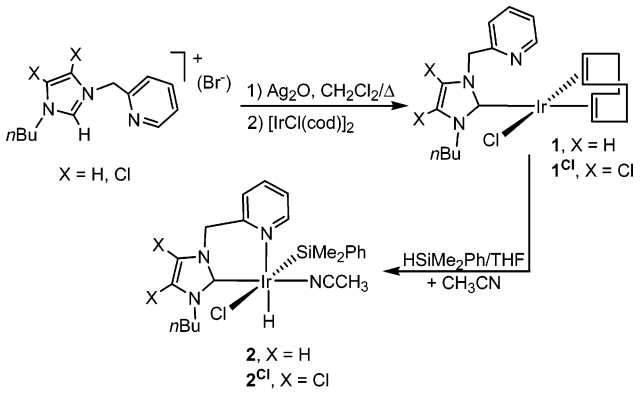

Results and Discussion

Synthesis of Compounds. The strategy for the preparation of complexes **1** and $\mathbf{1^{Cl}}$ was transmetalation from the previously obtained silver-NHC complexes.[14] The pyridine-imidazolium bromides were deprotonated with silver oxide to form the silver-NHC species, from which the carbene ligand was transmetalated to Ir by addition of $[IrCl(cod)]_2$ (Scheme 2).

Compound **1** was recently obtained in our group, although we proposed a structure with the chelate coordination of the pyridine-imidazolylidene ligand and a chloride as counterion of the cationic complex.[13] On the basis of the molecular structure of $\mathbf{1^{Cl}}$ determined by X-ray diffraction (see below), we now believe that the compound rather consists of a monodentate coordination of the NHC-ligand, with the chlorine atom completing a pseudo-square-planar coordination about the Ir(I) atom. The most significant feature of the NMR spectroscopic data of compound $\mathbf{1^{Cl}}$ is the signal due to the metalated carbene carbon, at 181.1 ppm, in the region where other metalated NHC complexes of Ir(I) appear,[11,15,16] thus confirming that the metalation has been produced.

Compounds **1** and $\mathbf{1^{Cl}}$ react with $HSiMe_2Ph$ (20 min in THF at room temperature) to provide the hydrido-silylated Ir(III) products, which were recrystallized in acetonitrile to provide compounds **2** and $\mathbf{2^{Cl}}$ in high yield. Compounds **2** and $\mathbf{2^{Cl}}$ coordinate the pyridine-imidazolylidene ligand in the chelate form, as confirmed by the molecular structure of $\mathbf{2^{Cl}}$ (see below). The most significant feature of the ^{1}H NMR spectroscopic data is the signal due to the hydride that appears at δ −19.8 for both **2** and $\mathbf{2^{Cl}}$. The coordination of the silyl group is confirmed by the appearance of the signals of the diastereotopic methyl groups at δ 0.11, 0.02 (**2**) and 0.19, 0.18 ($\mathbf{2^{Cl}}$). The $^{13}C\{^{1}H\}$ NMR spectra show the signals due to the metalated carbene carbon at δ 153.5 (**2**) and 152.2 ($\mathbf{2^{Cl}}$), in the region where other metalated NHC complexes of Ir(III) appear.[15,17] Both complexes **2** and $\mathbf{2^{Cl}}$ are air-stable products that can be handled under an air atmosphere and stored as solids without any special precaution.

(7) Bergens, S. H.; Noheda, P.; Whelan, J.; Bosnich, B. *J. Am. Chem. Soc.* **1992**, *114*, 2128. Maruyama, Y.; Yamamura, K.; Sagawa, T.; Katayama, H.; Ozawa, F. *Organometallics* **2000**, *19*, 1308. Adams, R. D.; Barnard, T. S. *Organometallics* **1998**, *17*, 2567. Maruyama, Y.; Yamamura, K.; Nakayama, I.; Yoshiuchi, K.; Ozawa, F. *J. Am. Chem. Soc.* **1998**, *120*, 1421. Esteruelas, M. A.; Herrero, J.; Oro, L. A. *Organometallics* **1993**, *12*, 2377. Itami, K.; Mitsudo, K.; Nishino, A.; Yoshida, J. *J. Org.* Chem. **2002**, *67*, 2645. Cervantes, J.; Gonzalez-AlaTorre, G.; Rohack, D.; Pannell, K. H. *Appl. Organomet. Chem.* **2000**, *14*, 146. Chung, L. W.; Wu, Y. D.; Trost, B. M.; Ball, Z. T. *J. Am. Chem. Soc.* **2003**, *125*, 11578. Crabtree, R. H. *New J. Chem.* **2003**, *27*, 771. Marciniec, B. *Coord. Chem. Rev.* **2005**, *249*, 2374. Lachaize, S.; Sabo-Etienne, S.; Donnadieu, B.; Chaudret, B. *Chem. Commun.* **2003**, 214.

(8) Faller, J. W.; D'Alliessi, D. G. *Organometallics* **2002**, *21*, 1743.

(9) Furmeier, S.; Griep-Raming, J.; Hayen, A.; Metzger, J. O. *Chem.-Eur. J.* **2005**, *11*, 5545. Furmeier, S.; Metzger, J. O. *J. Am. Chem. Soc.* **2004**, *126*, 14485. Santos, L. S.; Pavam, C. H.; Almeida, W. P.; Coelho, F.; Eberlin, M. N. *Angew. Chem., Int. Ed.* **2004**, *43*, 4330. Sabino, A. A.; Machado, A. H. L.; Correia, C. R. D.; Eberlin, M. N. *Angew. Chem., Int. Ed.* **2004**, *43*, 2514. Chen, H.; Zheng, X. B.; Yang, P. X.; Cooks, R. G. *Chem. Commun.* **2004**, 688. Meyer, S.; Koch, R.; Metzger, J. O. *Angew. Chem., Int. Ed.* **2003**, *42*, 4700. Zhang, X. Y.; Chen, P. *Chem.-Eur. J.* **2003**, *9*, 1852. Griep-Raming, J.; Meyer, S.; Bruhn, T.; Metzger, J. O. *Angew. Chem., Int. Ed.* **2002**, *41*, 2738. DePuy, C. H. *J. Org. Chem.* **2002**, *67*, 2393. Aliprantis, A. O.; Canary, J. W. *J. Am. Chem. Soc.* **1994**, *116*, 6985. Hwang, L. K.; Na, Y.; Lee, J.; Do, Y.; Chang, S. *Angew. Chem., Int. Ed.* **2005**, *44*, 6166. Guo, H.; Qian, R.; Liao, Y. X.; Ma, S. M.; Guo, Y. L. *J. Am. Chem. Soc.* **2005**, *127*, 13060. Qian, R.; Guo, H.; Liao, Y. X.; Guo, Y. L.; Ma, S. M. *Angew. Chem., Int. Ed.* **2005**, *44*, 4771. Santos, L. S.; Metzger, J. O. *Angew. Chem., Int. Ed.* **2006**, *45*, 977.

(10) Peris, E.; Crabtree, R. H. *C. R. Chimie* **2003**, *6*, 33. Peris, E.; Crabtree, R. H. *Coord. Chem. Rev.* **2004**, *248*, 2239.

(11) Mas-Marza, E.; Poyatos, M.; Sanau, M.; Peris, E. *Inorg. Chem.* **2004**, *43*, 2213.

(12) Poyatos, M.; Mas-Marza, E.; Mata, J. A.; Sanau, M.; Peris, E. *Eur. J. Inorg. Chem.* **2003**, 1215.

(13) Mas-Marza, E.; Sanau, M.; Peris, E. *Inorg. Chem.* **2005**, *44*, 9961.

(14) Wang, H. M. J.; Lin, I. J. B. *Organometallics* **1998**, *17*, 972. Garrison, J. C.; Youngs, W. J. *Chem. Rev.* **2005**, *105*, 3978. Lin, I. J. B.; Vasam, C. S. *Comments Inorg. Chem.* **2004**, *25*, 75.

(15) Viciano, M.; Poyatos, M.; Sanau, M.; Peris, E.; Rossin, A.; Ujaque, G.; Lledos, A. *Organometallics* **2006**, *25*, 1120.

(16) Mas-Marza, E.; Peris, E.; Castro-Rodriguez, I.; Meyer, K. *Organometallics* **2005**, *24*, 3158.

(17) Viciano, M.; Mas-Marza, E.; Poyatos, M.; Sanau, M.; Crabtree, R. H.; Peris, E. *Angew. Chem., Int. Ed.* **2005**, *44*, 444.

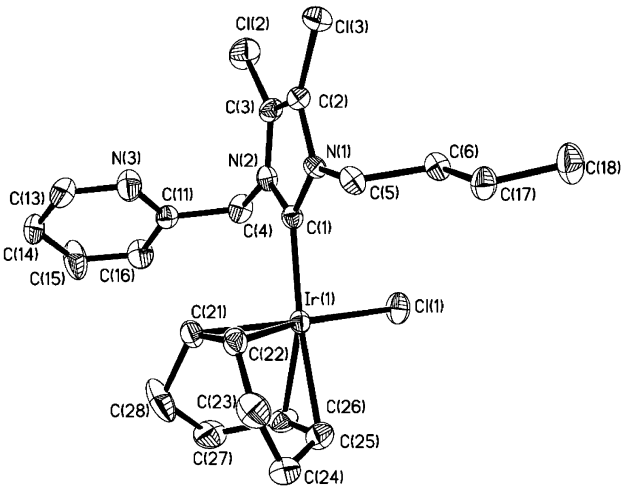

Figure 1. Molecular diagram of $\mathbf{1^{Cl}}$. Hydrogen atoms have been omitted for clarity. Selected bond (Å) lengths and angles (deg): Ir(1)−C(1) 2.012(8), Ir(1)−Cl(1) 2.377(2), C(3)−C(2) 1.313(12), C(1)−Ir(1)−Cl(1) 88.8(2).

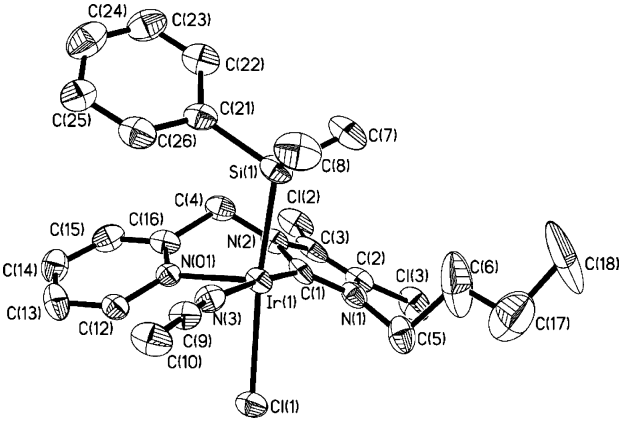

Figure 2. Molecular diagram of $\mathbf{2^{Cl}}\cdot CH_3OH$. Hydrogen atoms have been omitted for clarity. Selected bond (Å) lengths and angles (deg): Ir(1)−C(1) 1.950(9), Ir(1)−N(01) 2.163(7), Ir(1)−N(3) 2.058(8), Ir(1)−Si(1) 2.318(3), Ir(1)−Cl(1) 2.561(2), C(1)−Ir(1)−N(01) 87.9(3), Si(1)−Ir(1)−Cl(1) 171.91(9).

Molecular Structures of $\mathbf{1^{Cl}}$ and $\mathbf{2^{Cl}}$. The molecular structures of $\mathbf{1^{Cl}}$ and $\mathbf{2^{Cl}}$ were confirmed by single-crystal X-ray diffraction analysis. Figure 1 shows the molecular diagram of $\mathbf{1^{Cl}}$. The Ir atom adopts a pseudo-square-planar geometry with a monodentate coordination of the imidazolylidene ligand and the chloro and 1,5-cyclooctadiene completing the coordination sphere. The Ir−$C_{carbene}$ bond distance is 2.012(8) Å, lying in the range of other Ir-NHC complexes,[17,18] although in the lower limit. The mean Ir−C_{COD} distance is 2.183 Å trans to the NHC and 2.104 Å trans to chlorine, as a consequence of the higher trans influence of the carbene. The N(2)−C(1)−Ir(1)−Cl(1) torsion angle [78.9(7)°] indicates that the azole ring is quasi-orthogonal to the coordination plane of the molecule.

The molecular diagram of complex $\mathbf{2^{Cl}}$ is shown in Figure 2. The molecule consists of a severely distorted octahedral arrangement about the Ir atom. The Ir−$C_{carbene}$ distance is 1.950(9) Å, sligthly shorter than for other related Ir-NHC complexes,[17,18] probably due to the presence of the two electron-attracting choro substituents in the azole ring. This effect is in agreement with a previously reported work by Nolan and co-workers on a 4,5-dichloro-substituted-NHC coordinated to Ru; the shortening of the Ru−$C_{carbene}$ distance was interpreted in terms of the modification of the π-accepting capability of the ligand by the introduction of the two electron-withdrawing substituents.[19] The silyl and chlorine ligands adopt a trans disposition at a Si(1)−Ir(1)−Cl(1) angle of 171.91(9)°. The bite angle of the chelate ligand is 87.9(3)°. A close analysis of the structure indicates that the nonlocated hydride ligand must be trans to the pyridine ligand. The Ir(1)−N(01) bond distance [2.163(7) Å] is sligthly elongated with respect to other Ir-pyr complexes due to the trans influence of the hydride ligand.

Hydrosilylation Mechanistic Studies. We recently reported the catalytic properties of compound **1** toward hydrosilylation of terminal alkynes.[13] This complex showed low efficiency in terms of reaction yields, selectivity, and rates. In addition, the use of **1** in the reaction of phenylacetylene with $HSiMe_2Ph$ yielded a small amount of styrene (<10%), obviously produced by the mechanism implying the silylation process, which would also provide equimolecular amounts of $PhC{\equiv}CSiMe_2Ph$. Compound $\mathbf{1^{Cl}}$ and its hydrosilylated derivative $\mathbf{2^{Cl}}$ were also tested in the hydrosilylation of terminal alkynes, and their catalytic activities were similar to those provided by the nonchlorinated species **1** and **2**. This, in fact, can be considered as a very poor result in terms of catalyst design, but we thought that we could use compounds **1** and **2** in a series of experiments designed to give some light on the mechanism of hydrosilylation of acetylenes and the side reaction derived from the silylation process. The mechanistic studies could also be made by using the chlorinated complexes $\mathbf{1^{Cl}}$ and $\mathbf{2^{Cl}}$, but the isotopic distribution patterns resulting from the introduction of two chloro substituents would result in much more complicated ESI mass spectra. As mentioned above, **1** showed some activity toward this reaction, but its slow performance may be used to capture reaction intermediates by spectroscopic techniques and establish those reaction patterns that determine the production of the hydrosilylation or dehydrogenative silylation species.

Preliminary experiments were conducted by reacting stoichiometric amounts of **1** with $HSiMe_2Ph$ at 60 °C in acetonitrile. Under these conditions, exclusive formation of the silyl hydride **2** was completed after 20 min (Scheme 2). Conversely, the ESI-MS of an acetonitrile solution of complex **1** (showing the peak corresponding to $[\mathbf{1} - Cl]^+$) remains largely unchanged upon addition of increasing amounts of the acetylene derivatives at identical conditions. These results suggest that the catalytic reaction is triggered via formation of the silyl metal hydride, **2**. Subsequent experiments were tested by reacting different ratios of $HSiMe_2Ph$, acetylene derivatives, and complexes **1** and **2** at temperatures ranging from 40 to 80 °C. Under these conditions, the composition of the cationic intermediates changed drastically with time and temperature, and optimal conditions were found at 60 °C, at which evolution of the intermediates reached a steady state after 10 h. The operating conditions of the mass spectrometer were also optimized. The values of the desolvation and source temperature as well as the capillary voltage had a negligible effect on the abundance of the intermediates detected. However, the cone voltage was necessarily kept to a low value (5 V) to control the extent of fragmentation of the species observed. At these gentle conditions the intermediates identified appeared typically with various degrees of solvent coordination, therefore resulting in very crowded ESI mass spectra. Two

(18) Miecznikowski, J. R.; Crabtree, R. H. *Organometallics* **2004**, *23*, 629. Chianese, A. R.; Kovacevic, A.; Zeglis, B. M.; Faller, J. W.; Crabtree, R. H. *Organometallics* **2004**, *23*, 2461.

(19) Huang, J. K.; Schanz, H. J.; Stevens, E. D.; Nolan, S. P. *Organometallics* **1999**, *18*, 2370.

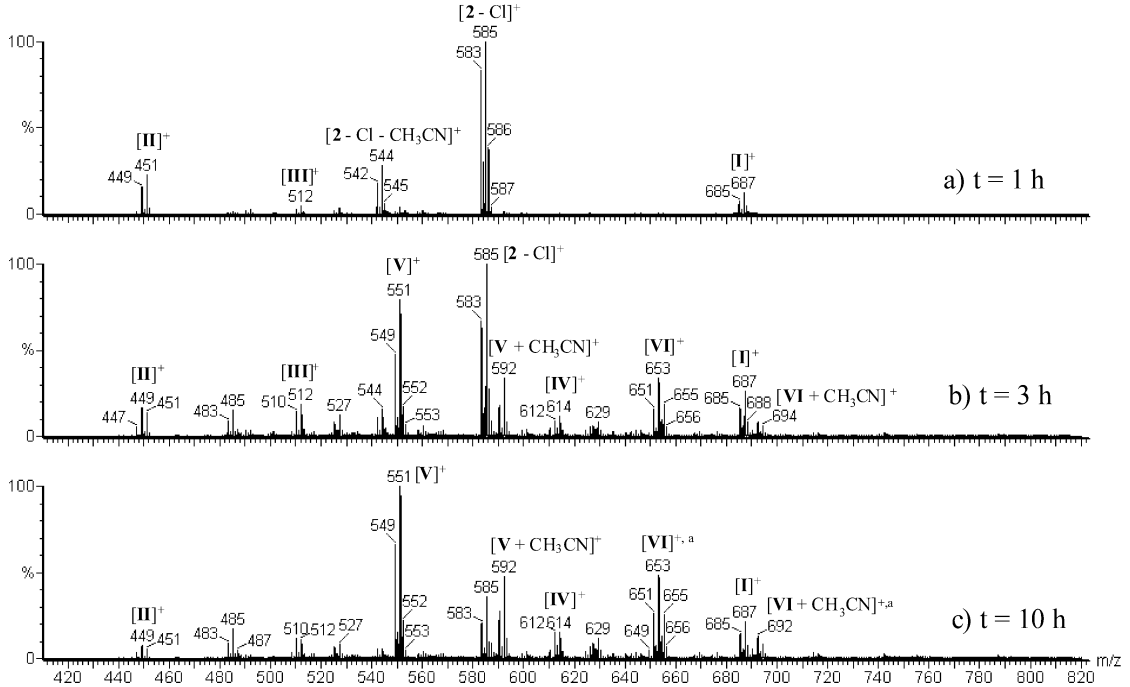

Figure 3. ESI-MS of the reaction of **2** with 2 equiv of phenylacetylene. $T = 60$ °C, CH_3CN, at three different reaction times. (a) The small signals due to species $[\mathbf{IV} + CH_3CN]^+/[\mathbf{IV} + 2CH_3CN]^+$ appear overlapped with $[\mathbf{VI}]^+/[\mathbf{VI} + CH_3CN]^+$.

different experiments are described in detail in this study, from which a mechanistic picture of the catalytic cycle is clearly seen: (i) reaction of a solution of **2** with a 2-fold excess of phenylacetylene at 60 °C and (ii) reaction of a solution of **1** with a 5-fold excess of both phenylacetylene and the silane at 60 °C. Typically, 100 μL was taken from the mixture at intervals of 30 min and cooled to room temperature in order to quench the reaction. Each aliquot was diluted with acetonitrile to a final concentration of approximately 5×10^{-5} M (based on the catalyst) and introduced directly to the ESI source.

(i) Reaction of Compound 2 with a 2-Fold Excess of Phenylacetylene. The reaction was monitored by both ESI-MS and ^{1}H NMR spectroscopy. The NMR analysis alone of the reaction gave little information about the reaction intermediates formed along the reaction process, but allowed us to confirm that, under these reaction conditions, the reaction was highly selective in the dehydrogenative-silylation process, since styrene was the only product observed (the signals due to PhC≡CSiMe$_2$-Ph are very difficult to assign by ^{1}H NMR spectroscopy in such a reaction medium). Figure 3 shows the mass spectra of the reaction at different intervals.

After 1 h (Figure 3a) three prominent peaks corresponding to species assigned to $[\mathbf{I}]^+$, $[\mathbf{II}]^+$, and $[\mathbf{III}]^+$ (see Scheme 3) are observed along with the intact $[\mathbf{2} - Cl]^+$ and $[\mathbf{2} - CH_3CN - Cl]^+$ starting precursors. The peak due to $[\mathbf{I}]^+$ (see ESI, Table 1S for the accurate mass determination) corresponds to the formal addition of one phenylacetylene molecule to $[\mathbf{2} - Cl]^+$. Species $[\mathbf{II}]^+$ is clearly assigned to the product that results from the release of the alkynylsilane, giving direct evidence of the presence of a dihydride complex as key intermediate resulting from the formation of alkynilsilanes. The putative ion $[\mathbf{III}]^+$ corresponds to the replacement of one acetonitrile by a phenylacetylene molecule on $[\mathbf{II}]^+$.

With the mass measurement alone, intermediate $[\mathbf{I}]^+$ may correspond to three different intermediates due to the π-coordination of phenylacetylene $[\mathbf{Ia}]^+$, insertion into the Ir−Si bond providing the alkenylsilane $[\mathbf{Ib}]^+$, or π-coordinated alkynylsilane $[\mathbf{Ic}]^+$ resulting from the β-elimination of the alkenylsilane in $[\mathbf{Ib}]^+$ (Scheme 4). In fact, the reaction mechanism is clearly dependent on whether $[\mathbf{Ia}]^+$ evolves to $[\mathbf{Ib}]^+$ to follow the hydrosilylation cycle or to $[\mathbf{Ic}]^+$ to give the silylation process (Scheme 4), as we will comment on below. To provide the alkynylsilane adduct $[\mathbf{Ic}]^+$, we believe that the acetylene inserts into the Ir−Si bond rather than into the Ir−H bond, as previously proposed.[6,8,20]

In the case of species $[\mathbf{III}]^+$, two intermediates are also possible, the one due to the π-coordination of PhC≡CH, $[\mathbf{IIIa}]^+$, and another that results from the insertion of phenylacetylene into the Ir−H bond, $[\mathbf{IIIb}]^+$. To further confirm the nature of these intermediates, tandem MS/MS experiments were carried out. Compound $[\mathbf{1} - Cl]^+$ dissociated, expelling the neutral

Table 1. Crystallographic Data of Compounds $\mathbf{1^{Cl}}$ and $\mathbf{2^{Cl}\cdot CH_3OH}$

	$\mathbf{1^{Cl}}$	$\mathbf{2^{Cl}}\cdot CH_3OH$
empirical formula	$C_{21}H_{27}Cl_3N_3Ir$	$C_{24}H_{31}Cl_3IrN_4OSi$
fw	620.01	718.17
wavelength	0.71073 Å	0.71073 Å
temperature	273(2) K	293(2) K
cryst syst	triclinic	triclinic
space group	$P\bar{1}$	$P\bar{1}$
a	10.3548(9) Å	11.221(7) Å
b	10.5700(9) Å	12.706(8) Å
c	11.0764(10) Å	13.236(8) Å
α	100.971(2)°	117.98(13)°
β	92.398(2)°	97.60(14)°
γ	108.656(2)°	105.83(14)°
V	1120.72(17) Å^3	1526.3(28) Å^3
Z	2	2
density (calcd)	1.837 Mg/m^3	1.563 Mg/m^3
abs coeff	6.326 mm^{-1}	4.698 mm^{-1}
no. od reflns collected	8055	7235
goodness-of-fit on F^2	1.110	1.106
final *R* indices	R1 = 0.0448	R1 = 0.0381
[$I > 2\sigma(I)$]	wR2 = 0.1170	wR2 = 0.0978

(20) Goikhman, R.; Milstein, D. *Chem.-Eur. J.* **2005**, *11*, 2983. Bosnich, B. *Acc. Chem. Res.* **1998**, *31*, 667. Ojima, I.; Clos, N.; Donovan, R. J.; Ingallina, P. *Organometallics* **1990**, *9*, 3127. Tanke, R. S.; Crabtree, R. H. *J. Am. Chem. Soc.* **1990**, *112*, 7984. Tanke, R. S.; Crabtree, R. H. *J. Chem. Soc., Chem. Commun.* **1990**, 1056.

Scheme 3

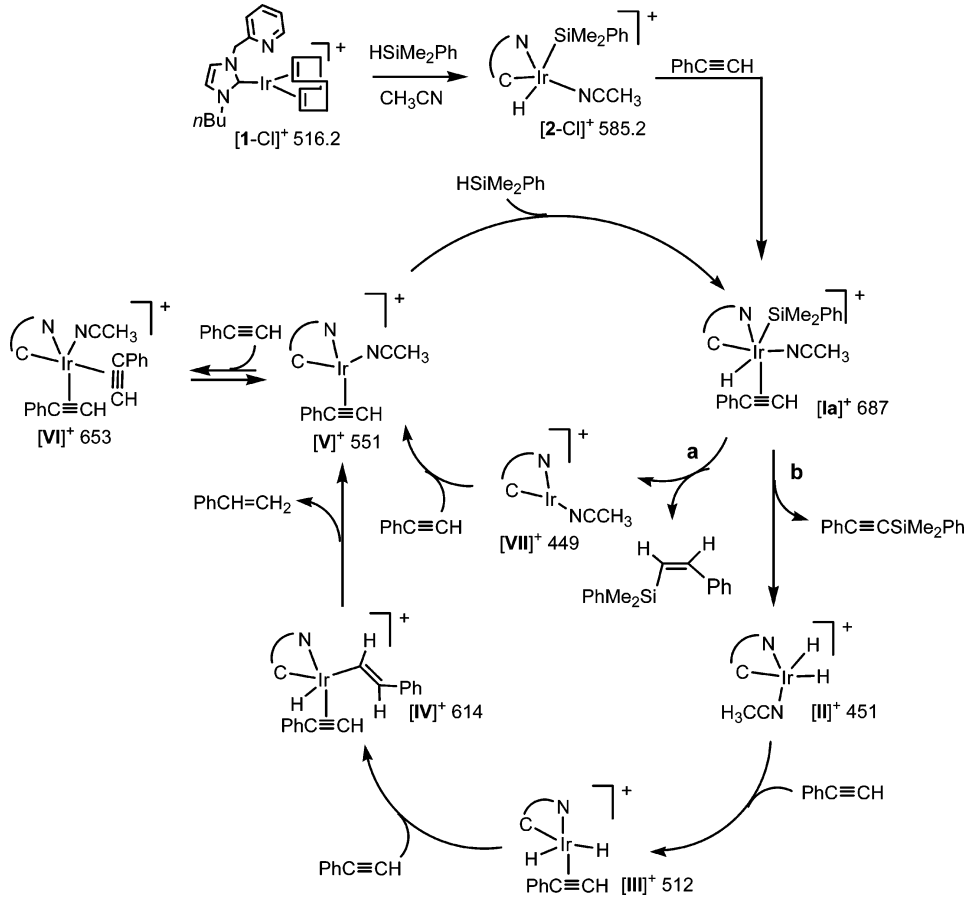

Scheme 4

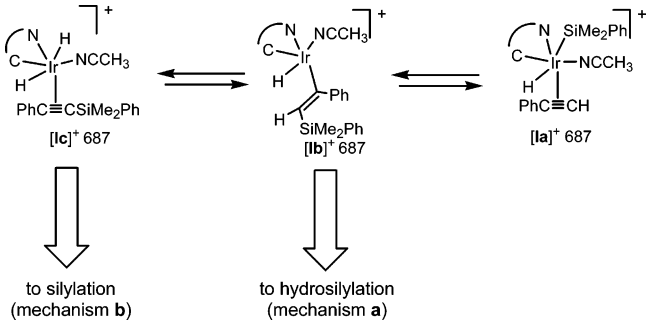

1,5-cyclooctadiene ligand followed by loss of H_2 (see Supporting Information), while compound $[\mathbf{2} - Cl]^+$ first eliminated the neutral acetonitrile and the fragment $HSiMe_2Ph$ via reductive elimination, followed by expulsion of H_2. This latter fragmentation channel seems to be a characteristic dissociation pattern of the {[*N*-*n*-butyl-*N*′-(2-pyridylmethyl)imidazole-2-ylidene]iridium}$^+$ moiety and has also been observed in related complexes.[21] Relevant information on the molecular organization of intermediates $[\mathbf{I}]^+$ and $[\mathbf{III}]^+$ is also extracted from these experiments. Species $[\mathbf{I}]^+$ fragments losing one acetonitrile followed by phenylacetylene plus molecular hydrogen and a final fragmentation channel evolving the $HSiMe_2Ph$ via reductive elimination. Therefore, species $[\mathbf{Ia}]^+$ could be tentatively assigned to the longer-living intermediate species and the subsequent steps involving $[\mathbf{Ib}]^+$ and $[\mathbf{Ic}]^+$ as a transient (nondetected) species leading to the hydrosilylation and silylation cycles. Species $[\mathbf{III}]^+$ fragments in a similar way, expelling one phenlyacetylene plus two hydrogen molecules. This fragmentation pathway might account for the presence of either species $[\mathbf{IIIa}]^+$ or $[\mathbf{IIIb}]^+$ since reductive elimination of one hydride and the alkenyl ligand occurring in the collision cell cannot be definitively ruled out. After 3 h (Figure 3b), the intensity of the peaks due to species $[\mathbf{I}]^+$, $[\mathbf{II}]^+$, and $[\mathbf{III}]^+$ increases relative to the abundance of the unperturbed compound $[\mathbf{2} - Cl]^+$. New species, namely, $[\mathbf{IV}]^+/[\mathbf{IV} + CH_3CN]^+$, $[\mathbf{V}]^+/[\mathbf{V} + CH_3CN]^+$, and $[\mathbf{VI}]^+/[\mathbf{VI} + CH_3CN]^+$, are distinguishable in the ESI mass spectra. Peaks assigned to $[\mathbf{IV}]^+/[\mathbf{IV} + CH_3CN]^+$ are observed as minor signals corresponding to the formal addition of an additional phenylacetylene molecule to $[\mathbf{III}]^+$. Peaks due to species $[\mathbf{V}]^+/[\mathbf{V} + CH_3CN]^+$ become dominant and are assigned to the release of styrene from species $[\mathbf{IV}]^+$ and coordination of one acetonitrile, thus completing the catalytic cycle. Additionally, a group of two signals ($[\mathbf{VI}]^+/[\mathbf{VI} + CH_3CN]^+$) due to the addition of one phenylacetylene molecule to species $[\mathbf{V}]^+$ are observed. The peaks due to $[\mathbf{IV} + CH_3CN]^+$ and $[\mathbf{VI}]^+$ are overlapped since their mass-to-charge ratio differs only by two units, although they are clearly distinguished due to the loss of the characteristic pattern indicative of the presence of one iridium atom. After 10 h (Figure 3c), the presence of all species is distinguished in the ESI-MS, $[\mathbf{V}]^+$ and $[\mathbf{VI}]^+$ being clearly dominant, while the relative abundance of compound $[\mathbf{2} - Cl]^+$ is dramatically reduced.

The monitoring of the reaction by ^{1}HNMR spectroscopy was also useful when compared to the data resulting from ESI-MS and the reaction mechanism proposed in Scheme 3. The hydride region of the spectrum showed signals that could be attributed to up to nine different species containing Ir−H bonds, and the

(21) Hinderling, C.; Plattner, D. A.; Chen, P. *Angew. Chem., Int. Ed. Engl.* **1997**, *36*, 243.

aliphatic region of the spectra did not allow any further information about the species present in the mixture. However, the spectroscopic patterns of the two cis-dihydrides $[\mathbf{II}]^+$ and $[\mathbf{III}]^+$ could clearly be detected among the rest of the signals, with resonances appearing at −20.9, −21.9 ppm ($^2J_{H-H} = 7.6$ Hz) and −17.8, −19.0 ppm ($^2J_{H-H} = 9.9$ Hz).

Experiments carried out with stoichiometric amounts of phenylacetylene and compound $[\mathbf{2} - Cl]^+$ showed that the nature of the intermediates detected was identical to that described above, with the only difference of a lower tendency to form $[\mathbf{VI}]^+$ as final product being observed, obviously because the lack of excess phenylacetylene would prevent the formation of $[\mathbf{VI}]^+$.

On the basis of the nature of the intermediate captured by ESI-MS, a plausible mechanism can be envisioned as a result of a first coordination of phenylacetylene to compound $[\mathbf{2} - Cl]^+$, followed by the expulsion of the alkynylsilane to give the dihydride intermediate $[\mathbf{II}]^+$. Further coordination of two molecules of phenylacetylene is accompanied by the hydrogenation of the alkyne to give species $[\mathbf{V}]^+$, which can be proposed as the active catalyst. Scheme 3 depicts this mechanism. The stereochemistry of the reaction intermediates is, of course, temptative.

The use of phenylacetylene as substrate does not provide information on the products formed, since it undergoes formation of apolar compounds nondetectable by ESI-MS. To overcome this limitation, we also tested the 4-aminophenylacetylene as substrate in order to get a complete picture of both the metal intermediate and the organic compounds formed under our experimental conditions. In this case the reaction reached a steady state after 6 h and the nature of the intermediates detected was quite similar to those with phenylacetylene (see Supporting Information, Figure 2S). This strategy provides key information on the composition of metal intermediates and organic substrates at each interval of time, thus allowing intermediates to be associated with the formation of organic compounds. For example, after 1 h the presence of a prominent peak at *m*/*z* 252.1 amu due to the formation of the protonated alkynilsilane NH_2-PhC≡$CSiMe_2$Ph was detected, in accordance with the mechanism proposed in Scheme 3, while no detection of 4-aminophenylethene was detected at this point. The formation of 4-aminophenylethene was observed after 3 h, along with the formation of species $[\mathbf{V}]^+$ and $[\mathbf{VI}]^+$. In the final stage of the reaction, only the protonated molecules of the starting 4-aminophenylacetylene, 4-aminophenylethene, and the alkynilsilane NH_2PhC≡$CSiMe_2$Ph were observed along with $[\mathbf{V}]^+$ and $[\mathbf{VI}]^+$. It must be pointed out that, under these conditions, $[\mathbf{2} - Cl]^+$ showed an extraordinary high selectivity toward the formation of dehydrogenative-silylated products, thus providing a unique scenario to study its mechanism with no competitive reactions. To our knowledge, there is only one report in the literature where this reaction occurs selectively, without the formation of other undesired alkenylsilane products,[5] although there are other examples in which the formation of the dehydrogenative-silylated products is achieved by using basic metal hydrides as reducing agents.[22] Interestingly, the products resulting from the dehydrogenative silylation are difficult to detect if reactions are followed by ^{1}H NMR spectroscopy, since the products are very easy to miss. The formation of styrene as hydrogen-trapping agent is the clearest indication that this process is occurring. In 1993 Crabtree and co-workers made a detailed study on the process and showed that many classical hydrosilylating catalysts also afforded the products resulting from the dehydrogenative silylation. In their paper, Crabtree and co-workers experimentally showed that the dehydrogenative silylation products are favored by increasing the alkyne/silane ratio.[6] Our proposed mechanism clearly supports this statement, since the dehydrogenative silylation needs a 2:1 molar ratio based on the silane: acetylene ratio to generate the reaction products (styrene and PhC≡$CSiMe_2$Ph). Besides, if we consider that $[\mathbf{Ia}]^+$ is the key intermediate for the reaction to proceed by mechanism a or b (Scheme 3), it is possible that the three type $[\mathbf{I}]^+$ intermediates (namely, $[\mathbf{Ia}]^+$, $[\mathbf{Ib}]^+$, and $[\mathbf{Ic}]^+$) are in equilibrium, and the presence of an excess of an alkyne (phenylacetylene) may favor the formation of the species $[\mathbf{III}]^+$ by displacing the coordinated alkynylsilane from $[\mathbf{Ic}]^+$, in a quasi-irreversible step.

(ii) Reaction of 1 and a 5-Fold Excess of Phenylacetylene and Silane. This reaction was also monitored by ESI-MS and ^{1}H NMR spectroscopy. Again, NMR spectroscopy was only useful in terms of monitoring the formation of the reaction products, but the detection of reaction intermediates was almost impossible due to the highly crowded spectra. Figure 4 shows the mass spectra of the reaction at different intervals. With this reaction we tried to simulate the catalytic conditions for the hydrosilylation of phenylacetylene, and hence, under these conditions, the reaction implies the use of a 20 mol % of catalyst.

After 1 h, the ESI-MS showed the presence of some unreacted compound $[\mathbf{1} - Cl]^+$, compound $[\mathbf{2} - Cl]^+$, and the presence of a new intermediate $[\mathbf{VII}]^+$, which coexists with $[\mathbf{III}]^+$ (all species are referenced in Scheme 3). Species $[\mathbf{VII}]^+$ is assigned to the product resulting from the hydrosilylation of the phenylacetylene and implies that at this point both hydro- and silylation mechanisms are simultaneously operative. The small mass difference between $[\mathbf{II}]^+$ and $[\mathbf{VII}]^+$ results in overlapped signals and the loss of the characteristic isotopic distributions due to the presence of iridium (^{191}Ir:^{193}Ir of 0.59:1.00). The signal due to species $[\mathbf{VII}]^+$ appears overlapped with $[\mathbf{II}]^+$. Nevertheless, the accurate mass measurements of species $[\mathbf{VII}]^+$ on the nonoverlapped isotopologue containing ^{191}Ir confirmed unambiguosly its molecular formula. This subtle difference represents the key step to distinguish between both hydro- and silylation pathways and must be observed in all cases where hydro- and silylation occur simultaneously, although when dealing with catalysts containing multiple isotope atoms such as palladium, ruthenium, chlorine, or bromine, the overlapping should not be so clearly distinguished.

After 3 and 10 h, the presence of intermediates $[\mathbf{I}]^+$, $[\mathbf{III}]^+$, $[\mathbf{IV}]^+$ (very small peak), $[\mathbf{V}]^+$, and $[\mathbf{VI}]^+$ is also detected. It is interesting to point out that under our catalytic conditions the starting compound **1** is present after the reaction mixture reached the steady state. Regarding the mechanistic picture shown in Scheme 3, this experimental evidence may be interpreted as a more favorable consumption of the silane through intermediate $[\mathbf{V}]^+$ rather than **1**.

Additionally, the presence of the hydrosilylation product was further confirmed by using 4-aminophenylacetylene as substrate, which results in the formation of the alkenylsilane H_2NPhHC═CHSiMe_2Ph, the alkynylsilane NH_2PhC≡$CSiMe_2$Ph, and NH_2-PhCH═CH_2 (see Supporting Information, Figure 3 S).

Conclusions

With this work we have shown that ESI-MS is a useful tool for the detection of the catalytic intermediates of the hydrosilylation/silylation of acetylenes in true catalytic conditions. Although ESI-MS can provide information only about the

(22) Itoh, M.; Kobayashi, M.; Ishikawa, J. *Organometallics* **1997**, *16*, 3068. Ishikawa, J.; Inoue, K.; Itoh, M. *J. Organomet. Chem.* **1998**, *552*, 303.

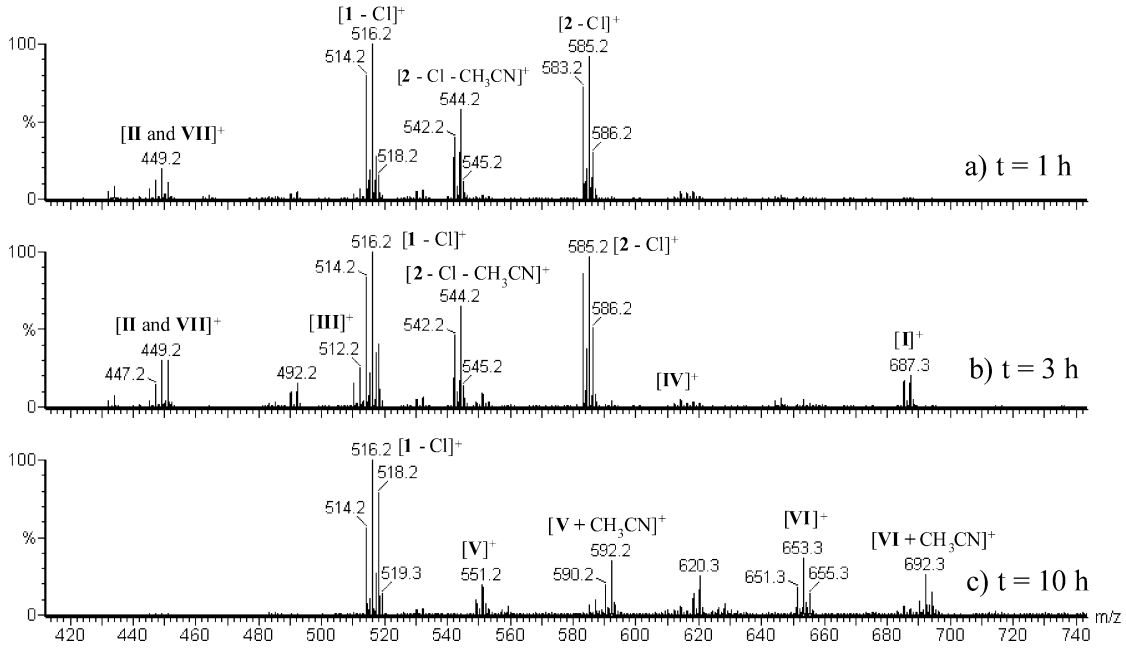

Figure 4. ESI-MS of the reaction of **1** with 5 equiv of phenylacetylene and 5 equiv of $HSiMe_2Ph$. $T = 60$ °C, CH_3CN, at three different reaction times. The small signal due to species $[\mathbf{VII}]^+$ appears overlapped with $[\mathbf{II}]^+$. The overlapping is clearly seen from the loss of the characteristic isotopic distributions due to the presence of iridium (^{191}Ir:^{193}Ir of 0.59:1.00).

molecular formulas of the species present in the reaction mixture, tandem MS/MS has allowed the confirmation of the molecular organization of most of the species present. The combination of this technique with ^1H NMR spectroscopy afforded a unique tool for the characterization of all the intermediates. In any case, we are aware that the species detected by ESI-MS may have been modified during the ionization process and may be slightly different from the true species present in the catalytic cycle. Regarding the active catalytic species involved in the catalytic cycle, we are aware that homogeneous catalysis can take place under the influence of minor (not detected) highly reactive species. In any case, the intermediates that we have detected are those expected for this well-known reaction.

As previously reported,[6] the presence of an excess of phenylacetylene favors the reaction to proceed by the silylation mechanism, thus yielding styrene and the corresponding alkynylsilane. We have rationalized this process in terms of a dynamic equilibrium between the reaction intermediates $[\mathbf{Ia}]^+$, $[\mathbf{Ib}]^+$, and $[\mathbf{Ic}]^+$, the latter two leading to the hydrosilylation and silylation cycles, respectively. The addition of an excess of acetylene would imply the replacement of the alkynylsilane ligand from $[\mathbf{Ic}]^+$ (to provide $[\mathbf{II}]^+$) in a pseudoirreversible process leading to the silylated products (pathway b in Scheme 3).

To our knowledge, this is the first time that all the reaction intermediates of the hydrosilylation/silylation of acetylenes have been spectroscopically and spectrometrically detected in true catalytic conditions.

Experimental Section

NMR spectra were recorded on Varian Mercury 300 and Inova 500 MHz spectrometers, using $CDCl_3$, CD_3CN, and DMSO-d_6 as solvents. Elemental analyses were carried out in an EA 1108 CHNS-O Carlo Erba analyzer. (*N*-*n*-Butyl)-4,5-dichloroimidazole,[23] chloro[*N*-*n*-butyl-*N*′-(2-pyridylmethyl)imidazole-2-ylidene](1,5-cyclooctadiene)iridium(I),[13] and $[IrCl(cod)]_2$[24] were synthesized according to literature procedures. All other reagents are commercially available and were used as received.

Synthesis of *N*-*n*-Butyl-*N*′-(2-pyridylmethyl)-4,5-dichloroimidazolium Bromide. A mixture of (*N*-*n*-butyl)-4,5-dichloroimidazole (1 g, 5.18 mmol) and 2-(bromomethyl)pyridine hydrobromide (1.30 g, 5.14 mmol) was kept neat at 110 °C overnight. Then, the reaction mixture was allowed to cool to room temperature, CH_2Cl_2 was added, and a yellow solid appeared. The solid was filtered (1.65 g) and dissolved in CH_3OH, and Na_2CO_3 (1 g, 9.43 mmol) was added in order to neutralize the HBr. The mixture was stirred at room temperature during 4 h (the solution turned from yellow to deep red). The excess Na_2CO_3 was filtered, the solution dried over Na_2SO_4, and the solvent eliminated under reduced pressured. The reaction mixture was dissolved in CH_2Cl_2 and the impurities were filtered off. The volatile components were removed under vacuum, obtaining the compound as a brown oil. Yield: 1.65 g, 90%. ^1H NMR (DMSO-d_6, 300 MHz): δ 9.81 (s, 1H, $NCHN_{imid}$), 8.53 (d, 1H, $^3J_{H-H} = 4.5$ Hz, H_{py}), 7.91 (t, 1H, $^3J_{H-H} = 7.6$ Hz, H_{py}), 7.60 (d, 1H, $^3J_{H-H} = 8.1$ Hz, H_{py}), 7.41 (m, 1H, H_{py}), 5.71 (s, 2H, $CH_{2linker}$), 4.31 (t, 2H, $^3J_{H-H} = 7.2$ Hz, $NCH_{2(n-Bu)}$), 1.81 (m, 2H, $CH_{2(n-Bu)}$), 1.35 (m, 2H, $CH_{2(n-Bu)}$), 0.93 (t, 3H, $^3J_{H-H} = 7.5$ Hz, $CH_{3(n-Bu)}$). $^{13}C\{^1H\}$ NMR (DMSO-d_6, 75 MHz): δ 152.6 (C_{py}), 150.3 (C_{py}), 138.3 (C_{py}), 137.9 ($NCHN_{imid}$), 124.5 (C_{py}), 123.2 (C_{py}), 120.0 ($Cl-C_{imid}$), 119.4 ($Cl-C_{imid}$), 52.8 ($CH_{2linker}$), 49.1 ($NCH_{2(n-Bu)}$), 30.9 ($CH_{2(n-Bu)}$), 19.4 ($CH_{2(n-Bu)}$), 14.0 ($CH_{3(n-Bu)}$). Anal. Calcd for $C_{13}N_3H_{16}Cl_2Br$ (MW 365.10): C, 42.77; H, 4.42; N, 11.51. Found: C, 42.95; H, 4.33; N, 11.76. Electrospray MS (20 V, MeOH) *m*/*z*: 284.1 $[M^+]$.

Synthesis of Chloro[*N*-*n*-butyl-*N*′-(2-pyridylmethyl)-4,5-dichloroimidazole-2-ylidene](1,5-cyclooctadiene)iridium(I), $\mathbf{1^{Cl}}$. A mixture of Ag_2O (210 mg, 0.91 mmol) and *N*-*n*-butyl-*N*′-(2-pyridylmethyl)-4,5-dichloroimidazolium bromide (220 mg, 0.60 mmol) was refluxed in CH_2Cl_2 (10 mL) for 90 min. Then $[IrCl(cod)]_2$ (200 mg, 0.30 mmol) was added. The mixture was refluxed for 90 min and filtered through Celite, and the volatile components were removed under vacuum. The crude solid was redissolved in CH_2Cl_2, and the impurities were removed by precipitation with ether. The product $\mathbf{1^{Cl}}$ was washed with cold ether and dried under vacuum. Yield: 200 mg (54%). ^1H NMR ($CDCl_3$, 500 MHz): δ

(23) Corberan, R.; Sanau, M.; Peris, E. *J. Am. Chem. Soc.* **2006**, *128*, 3974.

(24) Lin, Y.; Nomiya, K.; Finke, R. G. *Inorg. Chem.* **1993**, *32*, 6040.

8.57 (d, 1H, $^3J_{H-H}$ = 5.0 Hz, H_{py}), 7.69 (t, 1H, $^3J_{H-H}$ = 7.5 Hz, H_{py}), 7.34 (d, 1H, $^3J_{H-H}$ = 8.0 Hz, H_{py}), 7.22 (m, 1H, H_{py}), 5.88 (d, 1H, $^2J_{H-H}$ = 15.5 Hz, $CH_{2linker}$), 5.53 (d, 1H, $^2J_{H-H}$ = 16.0 Hz, $CH_{2linker}$), 4.60 (m, 2H, CH_{COD}), 4.46 (t, 2H, $^3J_{H-H}$ = 8.5 Hz, $CH_{2(n-Bu)}$), 2.80 (m, 2H, CH_{COD}), 2.23−1.91 (brs, 4H, CH_{2COD}), 1.78 (m, 2H, $CH_{2(n-Bu)}$), 1.62 (m, 4H, CH_{2COD}), 1.50 (m, 2H, $CH_{2(n-Bu)}$), 1.04 (t, 3H, $^3J_{H-H}$ = 7.1 Hz, $CH_{3(n-Bu)}$). $^{13}C\{^1H\}$ NMR ($CDCl_3$, 125 MHz): δ 181.1 (C−Ir), 155.2 (C_{py}), 150.0 (C_{py}), 137.1 (C_{py}), 123.2 (C_{py}), 120.9 (C_{py}), 116.6 (Cl−C_{imid}), 116.4 (Cl−C_{imid}), 86.5 (CH_{COD}), 86.7 (CH_{COD}), 55.1 ($CH_{2linker}$), 51.8 (CH_{2COD}), 50.2 (CH_{2COD}), 50.0 ($CH_{2(n-Bu)}$), 32.7 (CH_{2COD}), 32.6 ($CH_{2(n-Bu)}$), 29.6 (CH_{2COD}), 20.3 ($CH_{2(n-Bu)}$), 13.9 ($CH_{3(n-Bu)}$). Anal. Calcd for $C_{21}H_{27}Cl_3N_3Ir$ (620.04): C, 40.68; H, 4.39; N, 6.78. Found: C, 40.54; H, 4.83; N, 6.65. Electrospray MS (25 V, CH_2Cl_2) *m*/*z*: 584.1 $[M - Cl]^+$.

Synthesis of [*N*-*n*-Butyl-*N*′-(2-pyridylmethyl)imidazole-2-ylidene](chloro)(hydrido)(dimethylphenylsilyl)(acetonitrile)-iridium(III), 2. To a solution of chloro[*N*-*n*-butyl-*N*′-(2-pyridylmethyl)imidazole-2-ylidene](1,5-cyclooctadiene)iridium(I) (100 mg, 0.16 mmol) in dried THF (5 mL) was added $HSiMe_2Ph$ (60 μL, 0.39 mmol). Then the mixture was stirred at room temperature for 20 min. During this time, a light yellow solid appeared. The solid was filtered and recrystallized from acetonitrile to afford a light yellow crystalline solid. Yield: 80 mg (71%). ^1H NMR (CD_3CN, 500 MHz): δ 9.25 (d, $^3J_{H-H}$ = 4.0 Hz, 1H, H_{py}), 7.81 (t, 1H, $^3J_{H-H}$ = 7.5 Hz, H_{py}), 7.37 (t, 1H, $^3J_{H-H}$ = 6.5 Hz, H_{py}), 7.27−7.23 (m, 3H, 1 H, H_{py}, 2H, ph_{silane}), 7.02 (m, 3H, ph_{silane}), 6.94 (s, 1H, CH_{imid}), 6.90 (s, 1H, CH_{imid}), 4.83 (d, 1H, $^2J_{H-H}$ = 15.0 Hz, $CH_{2linker}$), 4.70 (d, 1H, $^2J_{H-H}$ = 15.0 Hz, $CH_{2linker}$), 3.91 (m, 2H, $CH_{2(n-Bu)}$), 1.80 (m, 2H, $CH_{2(n-Bu)}$), 1.50 (m, 2H, $CH_{2(n-Bu)}$), 1.06 (t, 3H, $^3J_{H-H}$ = 7.1 Hz, $CH_{3(n-Bu)}$), 0.11 (s, 3H, $CH_{3silane}$), 0.02 (s, 3H, $CH_{3silane}$), −19.78 (s, 1H, Ir−H). $^{13}C\{^1H\}$ NMR (CD_3CN, 75 MHz): δ 154.6 (C_{py}), 153.5 (C−Ir), 137.6 (C_{ph}), 133.2 (C_{imid}), 133.1 (C_{ph}), 129.42 (C_{ph}), 127.90 (C_{imid}), 126.8 (C_{ph}), 126.5 (C_{py}), 123.86 (C_{py}), 120.1 (C_{py}), 119.5 (C_{py}), 54.9 ($CH_{2linker}$), 50.4 ($CH_{2(n-Bu)}$), 31.8 ($CH_{2(n-Bu)}$), 20.0 ($CH_{2(n-Bu)}$), 13.4 ($CH_{3(n-Bu)}$), 5.2 ($CH_{3silane}$), 3.1 ($CH_{3silane}$). Anal. Calcd for $C_{23}H_{32}ClN_4IrSi$ (620,28): C, 44.54; H, 5.20; N, 9.03. Found: C, 445.76; H, 5.37; N, 8.92. Electrospray MS (15 V, CH_3CN) *m*/*z*: 585.2 $[M - Cl]^+$.

Synthesis of [*N*-*n*-Butyl-*N*′-(2-pyridylmethyl)-4,5-dichloroimidazole-2-ylidene](chloro)(hydrido)(dimethylphenylsilanure)-(acetonitrile), 2^{Cl}. To a solution of *N*-*n*-butyl-*N*′-(2-pyridylmethyl)-4,5-dichloroimidazole-2-ylidene](1,5-cyclooctadiene)iridium(I) (100 mg, 0.15 mmol) in dried THF (5 mL) was added $HSiMe_2Ph$ (60 μL, 0.39 mmol). Then the mixture was stirred at room temperature for 40 min. During this time a yellow solid appeared. The solid was filtered and recrystallized from acetonitrile to afford a light yellow crystalline solid. Yield: 50 mg (45%). ^1H NMR (CD_3CN, 500 MHz): δ 9.26 (s, 1H, H_{py}), 7.88 (t, 1H, $^3J_{H-H}$ = 7.5 Hz, H_{py}), 7.44 (t, 1H, $^3J_{H-H}$ = 7.5 Hz, H_{py}), 7.37 (m, 1H, H_{py}), 7.29 (m, 2H, ph_{silane}), 7.07 (m, 3H, ph_{silane}), 5.04 (d, 1H, $^2J_{H-H}$ = 15.5 Hz, $CH_{2linker}$), 4.61 (d, 1H, $^2J_{H-H}$ = 15.5 Hz, $CH_{2linker}$), 4.01 (m, 2H, $CH_{2(n-Bu)}$), 1.80 (m, 2H, $CH_{2(n-Bu)}$), 1.50 (m, 2H, $CH_{2(n-Bu)}$), 1.06 (t, 3H, $^3J_{H-H}$ = 7.1 Hz, $CH_{3(n-Bu)}$), 0.19 (s, 3H, $CH_{3silane}$), 0.18 (s, 3H, $CH_{3silane}$), −19.78 (s, 1H, Ir−H). $^{13}C\{^1H\}$ NMR (CD_3CN, 75 MHz): δ 154.6 (C_{py}), 152.2 (C−Ir), 137.9 (C_{ph}), 133.0 (C_{ph}), 126.9 (C_{ph}), 126.7 (C_{py}), 125.3 (C_{py}), 124.2 (C_{py}), 52.3 ($CH_{2linker}$), 49.2 ($CH_{2(n-Bu)}$), 30.9 ($CH_{2(n-Bu)}$), 20.1 ($CH_{2(n-Bu)}$), 13.4 ($CH_{3(n-Bu)}$), 3.9 ($CH_{3silane}$), 3.8 ($CH_{3silane}$). Anal. Calcd for $C_{23}H_{30}Cl_3N_4IrSi$ (689.17): C, 40.08; H, 4.39; N, 8.13. Found: C, 40.22; H, 4.17; N, 8.31. Electrospray MS (40 V, *m*/*z*): 653 $[M - Cl]^+$, 612.1 $[M - Cl - CH_3CN]^+$.

X-ray Diffraction Studies. Crystals for X-ray diffraction of $\mathbf{1^{Cl}}$ were obtained by slow diffusion of ether in a concentrated solution of the compound in CH_2Cl_2. Crystals for X-ray diffraction of $\mathbf{2^{Cl}}$ were obtained by slow evaporation of a concentrated solution of the compound in CH_3CN/CH_3OH (9:1). Crystal data are summarized in Table 1. Data collection was performed at room temperature on a Siemens Smart CCD diffractometer using graphite-monochromated Mo Kα radiation (λ = 0.71073 Å). The diffraction frames were integrated using the SAINT package.[25] Space group assignment was based on systematic absences, E statistics, and successful refinement of the structures. The structure was solved by direct methods with the aid of successive difference Fourier maps and were refined using the SHELXTL 6.1 software package.[26] All non-hydrogen atoms were refined anisotropically, and hydrogen atoms were assigned to ideal positions and refined using a riding model.

Electrospray Ionization Mass Spectrometry. A hybrid QTOF I (quadrupole-hexapole-TOF) mass spectrometer with an orthogonal Z-spray-electrospray interface (Micromass, Manchester, UK) was used. The drying gas as well as nebulizing gas was nitrogen at a flow of 400 and 80 L/h, respectively. The temperature of the source block was set to 100 °C and the desolvation temperature to 120 °C. Mass calibration was performed daily using a solution of sodium iodide in 2-propanol/water (50:50) from *m*/*z* 50 to 1500 amu. A capillary voltage of 3.5 kV was used in the positive scan mode, and the cone voltage was set to 5 V. Sample solutions were infused via syringe pump directly connected to the ESI source at a flow rate of 10 μL/min. ESI-MS monitoring of the reactions was carried out for three independent experiments, observing reproducibility in all cases. For the accurate mass measurements, a solution of 3,5-diiodotyrosine (ca. 1 mg/L used as lock mass fw = 433.8750 amu) in acetonitrile was infused simultaneously with the sample solution via a T-shaped connection directly connected to the ESI source. Accurate mass measurements were carried out on the most intense peak, corresponding to the isotopomer that contains ^{193}Ir. In those species appearing partially overlapped we chose the nonoverlapped isotopologue containing ^{191}Ir for the accurate mass determination. The values given in Table 1S correspond to three independent measurements. The observed isotopic pattern of each intermediate perfectly matched the theoretical isotope pattern calculated from their elemental composition using the MassLynx 4.0 program. Tandem MS/MS spectra were obtained at various collision energies (typically varied from 0 to 50 eV) by selecting the precursor ion of interest with the first quadrupole (Q1) with an isolation width of approximately 1 Da and scanning with the time-of-flight analyzer (TOF). Argon was used as collision gas, and the pressure in the collision cell was maintained at 4×10^{-5} mbar.

Acknowledgment. We gratefully acknowledge financial support from the MEC of Spain (projects CTQ2005-05187) and Bancaixa (P1.1B2004-07). E.M.-M. thanks the Spanish Ministerio de Educación y Ciencia for a fellowship.

Supporting Information Available: Crystallographic data in CIF format. ESI-MS of the hydrosilylation processes using 4-aminophenylacetylene. Accurate mass determinations, isotopic pattern analysis, and tandem MS/MS experiments for all intermediates detected. This material is available free of charge via the Internet at http://pubs.acs.org.

OM0602308

(25) *SAINT, Bruker Analytical X-ray System, version 5.0*; Bruker AXS: Madison, WI, 1998.

(26) Sheldrick, G. M. *SHELXTL, version 6.1*; Bruker AXS, Inc.: Madison, WI, 2000.